International Journal of Basic and Applied Sciences, 14 (1) (2025) 92-98

International Journal of Basic and Applied Sciences

Website: www.sciencepubco.com/index.php/IJBAS
https://doi.org/10.14419/gv4spa37
Research paper

Wireless interrogator for passive electromagnetic sensors for IoT applications

Anil M Kasture [1]*, Kailash J Karande [1], Shankar D Nawale [2], Altaf O Mulani [1]

[1] *Electronics and Telecommunication, SKN Sinhgad College of Engineering, Korti, Pandharpur, Dist Solapur, Maharashtra, India*
[2] *Electronics and Telecommunication, N B Navale Sinhgad College of Engineering, Kegaon, Solapur, Dist-Solapur, Maharashtra, India*
**Corresponding author E-mail: anilkasture01@gmail.com*

Received: March 19, 2025, Accepted: April 13, 2025, Published: April 24, 2025

Abstract

This work presents a novel wireless interrogator designed to efficiently interface with passive electromagnetic sensors, addressing critical challenges in energy efficiency and real-time IoT connectivity. The Internet of Things (IoT) is transforming a wide range of industries, enabling real-time monitoring and information collection through interconnected sensor networks. Passive electromagnetic sensors, which do not require an external power source, offer significant advantages in energy efficiency and maintenance-free operation. However, efficient data interrogation and communication from these sensors remain a challenge, particularly in IoT-based wireless applications. The design and development of a wireless IoT interrogator for passive electromagnetic sensors are described in this paper. The proposed interrogator leverages advanced wireless communication protocols and energy-efficient techniques to interrogate passive sensors, retrieve data, and transmit it to IoT networks for real-time monitoring and analysis. We analyze the system's performance through experiments, highlighting the interrogator's capability to support diverse IoT applications, such as environmental monitoring and smart agriculture. The proposed system is energy-efficient, scalable, and capable of supporting real-time data transmission to IoT networks, making it ideal for a wide range of IoT applications. F1 antenna gain is 3.50 dBi, and mF1 antenna gain is 5.10 dBi. Output power for frequency doubling reflectenna system observed -20dB, -89dB for distance between Tx and Rx at 100 cm, 1000cm, respectively.

Keywords: *Wireless IoT; Interrogator; Passive Electromagnetic Sensors; Energy Efficiency; Sensor Networks; Data Communication; IoT Application.*

1. Introduction

The IoT ecosystem consists of a vast number of devices and sensors interconnected to gather, process, and transmit data for various applications, ranging from smart cities and healthcare to agriculture and industrial automation [1 - 3]. Among these sensors, passive electromagnetic sensors, such as radio-frequency identification (RFID) tags and sensor transponders, have gained significant attention due to their ability to operate without an external power source [4 - 6]. These sensors are typically powered by the interrogation signal received from a reader, making them highly energy-efficient and ideal for long-term, low-maintenance deployments [7 - 9]. However, efficiently extracting data from passive electromagnetic sensors and integrating them into wireless IoT networks presents several challenges [10 - 12]. These challenges include the limited range of communication, interference from surrounding environments, and the need for low-power, robust interrogation systems capable of supporting diverse IoT applications [13 - 15]. Despite the advancements in wireless sensor technologies, current interrogation systems for passive electromagnetic sensors still face limitations, particularly in terms of communication range, energy efficiency, and the ability to integrate seamlessly into IoT networks [16 - 18]. The need for an efficient, reliable, and scalable wireless interrogator is critical for realizing the full potential of passive electromagnetic sensors in IoT applications. This paper proposes a wireless IoT interrogator that addresses these challenges, focusing on maximizing energy efficiency, increasing range, and ensuring seamless integration with IoT platforms. Figure 1 shows a frequency multiplying reflectenna with an Interrogator for an IoT application.

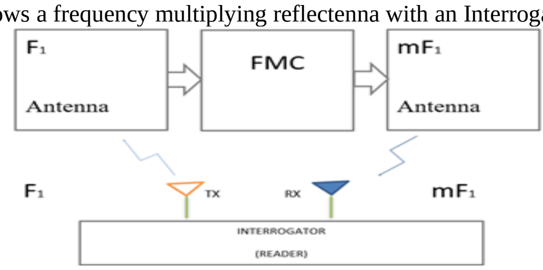

Fig. 1: Frequency Multiplying Reflectenna with Interrogator for IoT Application.

2. Proposed system

Several studies have explored the use of passive electromagnetic sensors and the development of interrogation systems for wireless IoT networks [19 - 21]. Most existing systems are based on RFID technology, which utilizes passive tags that are powered by the reader's interrogation signal. However, challenges such as limited communication range and power consumption remain prominent. In the past decade, research has focused on enhancing the performance of interrogators by using techniques like multiple-input multiple-output (MIMO) antennas, energy harvesting, and novel modulation schemes. Moreover, efforts have been made to integrate IoT protocols like MQTT and CoAP for seamless communication between sensors and cloud-based platforms. While significant progress has been made, the development of a wireless IoT interrogator for passive sensors that balances range, energy efficiency, and IoT compatibility remains a critical area of research [22],[23].
Use analytical formulas to estimate the initial dimensions of the microstrip patch antenna [24],[25],[26]. Key Parameters:
Patch Width (W), which is mentioned in equation number 1.

$$W = \frac{c}{2f_r}\sqrt{\frac{2}{\varepsilon_r+1}} \tag{1}$$

Where, c= speed of light (3×10^8 m/s),
f_r= resonant frequency (433 MHz),
ε_r= dielectric constant of the substrate.
Effective Dielectric Constant (ε_{reff}): which is calculated by equation number 2.

$$\varepsilon_{reff} = \frac{\varepsilon_r+1}{2} + \frac{\varepsilon_r-1}{2}\left[1+12\frac{h}{W}\right]^{-1/2} \tag{2}$$

Where, W= patch width,
h= substrate Material thickness,
ε_r= dielectric constant of the substrate.
$W/h \le 1$ use equations 3 and 4. If $W/h \ge 1$ use equations 5 and 6.

$$\varepsilon_{reff} = \frac{\varepsilon_r+1}{2} + \frac{\varepsilon_r-1}{2}\left[\left(1+12\frac{h}{W}\right)^{-0.5} + 0.04\left(1-\frac{W}{h}\right)^2\right] \tag{3}$$

$$Z_c = \frac{\eta}{2\pi\sqrt{\varepsilon_{reff}}}\ln\left(\frac{8h}{W}+0.25\frac{W}{h}\right) \tag{4}$$

$$\varepsilon_{reff} = \frac{\varepsilon_r+1}{2} + \frac{\varepsilon_r-1}{2}\left(1+12\frac{h}{W}\right)^{-0.5} \tag{5}$$

$$Z_c = \frac{\eta}{\sqrt{\varepsilon_{reff}}}\left[\frac{W}{h}+1.393+0.677\ln\left(\frac{W}{h}+1.444\right)\right]^{-1} \tag{6}$$

Patch Length (L): which is mentioned in equation number 7.

$$L = \frac{c}{2f_r\sqrt{\varepsilon_{reff}}} - 2\Delta L \tag{7}$$

Where, ΔL is the fringing field extension.
Fringing field extension (ΔL): which is calculated by equation number 8.

$$\Delta L = 0.412 * h * \frac{(\varepsilon_{reff}+0.3)\left(\frac{W}{h}+0.264\right)}{(\varepsilon_{reff}-0.258)\left(\frac{W}{h}+0.8\right)} \tag{8}$$

3. Implementation techniques

The wireless IoT interrogator proposed in this paper is designed to work with passive electromagnetic sensors that communicate through reflected signal. The system consists of three main components. Interrogator (Reader) is a wireless device responsible for transmitting interrogation signals, frequency multiplying reflectenna (FMR) and receiving reflected signal responses from passive sensors. FMR (Passive Sensors) are electromagnetic sensors that respond to the interrogation signal by reflecting signal to the sensor data. The interrogator communicates with the FMR passive sensor nodes over a wireless medium using wireless communication such as Wi-Fi, LoRa WAN etc. The design of the wireless IoT interrogator focuses on several critical factors. Since passive electromagnetic sensors do not have their power source, the interrogator must minimize energy consumption while maintaining reliable communication. The interrogator supports long-range operation to ensure the scalability of the IoT network. The interrogator must support high data throughput for real-time monitoring and efficient data retrieval from multiple sensor nodes simultaneously. The interrogator should be able to interface with popular IoT platforms and support standard communication protocols like MQTT, CoAP, and HTTP. The system should support the integration of multiple passive sensors across a large area, making it useful for applications such as asset tracking, environmental sensing, and industrial automation. The interrogator utilizes reflected signals to communicate with FMR passive sensor nodes. In reflected signal communication, the sensor signal is received from the interrogator and reflected. The interrogator receives the reflected signal to retrieve the data. A different structure for the 433 MHz frequency was designed and simulated. Figure 2 shows a 3-D radiation pattern with gain in (dBi) and the current distribution of a) Meander Line Monopole Antenna of 433 MHz, b) Meander Line Antenna of 433 MHz.

(A) (B)

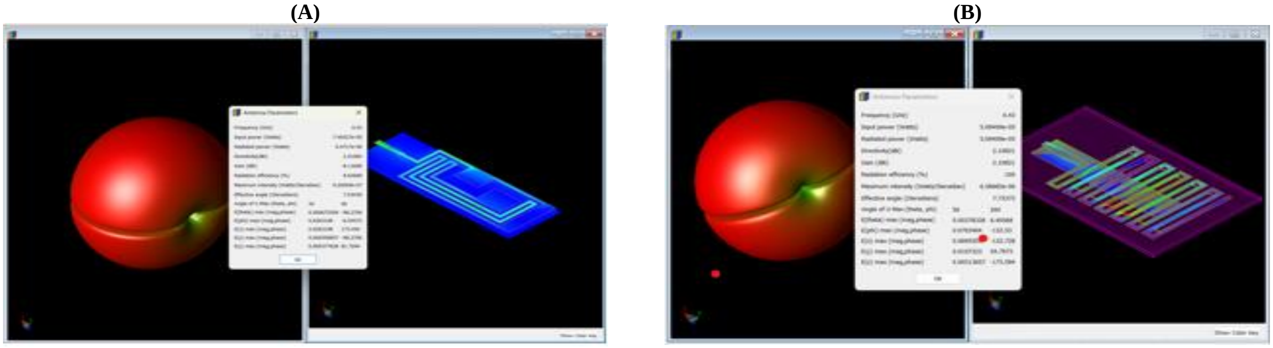

Fig. 2: 3-D Radiation Pattern with Gain in (Dbi) and Current Distribution of A) Meander Line Monopole Antenna of 433Mhz, B) Meander Line Antenna of 433Mhz.

(A) (B)

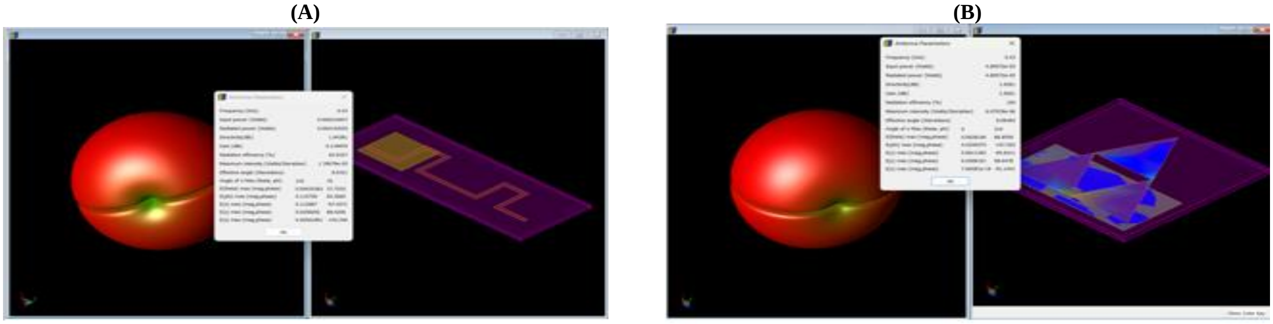

Fig. 3: 3-D Radiation Pattern with Gain in (DBI) and Current Distribution of A) Microstrip Antenna with Cohen-Minkowski Fractal of 433Mhz, B) Microstrip Antenna with Triangle Fractal of 433Mhz.

Figure 3 shows a 3-D radiation pattern with gain in (DBI) and current distribution of a) Microstrip Antenna with Cohen-Minkowski Fractal of 433Mhz, b) Microstrip Antenna with Triangle Fractal of 433Mhz. Figure 4 shows a) simulation of Microstrip Antenna, b) radiation pattern and gain of F1 Microstrip antenna for 433 MHz. After comparison of different Structure of 433 MHz antennas gain, we observed that gain of Microstrip Patch Antenna is more.

(A) (B)

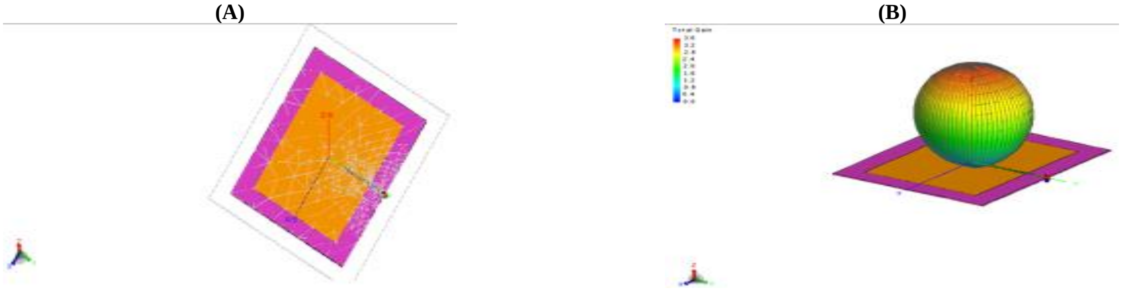

Fig. 4: A) Simulation of F1 Microstrip Antenna, B) Simulated Radiation Pattern and Gain of F1 Microstrip Antenna for 433 Mhz.

The following table I represents gain of different structures of Microstrip Patch Antenna of 433Mhz. The planner microstrip antenna is designed to operate at a fundamental frequency and exhibit a second-order nonlinearity, which is the key to achieving frequency doubling. F1 microstrip patch antenna serves as the primary radiating element, designed to operate at a fundamental frequency of F1.

Table 1: Represents Gain of Different Structures of Microstrip Patch Antenna of 433Mhz

Antenna Structure	Gain (DBI)
Meander Line Monopole Antenna	2.52
Meander Line Antenna	2.11
Microstrip Antenna with Cohen-Minkowski Fractal	1.94
Microstrip Antenna with Triangle Fractal	1.93
Microstrip Patch Antenna	3.50

Frequency multiplying reflectenna (FMC) converts the fundamental frequency to the mF1 frequency. Figure 5 shows the simulation circuit diagram of a frequency-doubling system using a Schottky diode, which is implemented in NI Multisim, that will convert the F1 frequency to 2F1 frequency. A different structure for the 866 MHz frequency was designed and simulated. Figure 6 shows a 3-D radiation pattern with gain in (dBi) and current distribution of a) Meander Line Monopole Antenna of 866 MHz, b) Meander Line Antenna of 866 MHz. Figure 7 shows a 3-D radiation pattern with gain in (dBi) and current distribution of a) Microstrip Antenna with Cohen-Minkowski Fractal of 866 MHz, b) Microstrip Antenna with Triangle Fractal of 866 MHz. Figure 8 shows a) simulation of the Microstrip antenna, b) radiation pattern, and gain of the mF1 Microstrip antenna for 866 MHz. After comparison of different structures of 866 MHz antennas' gain, we observed that the gain of the Microstrip Patch Antenna is higher.

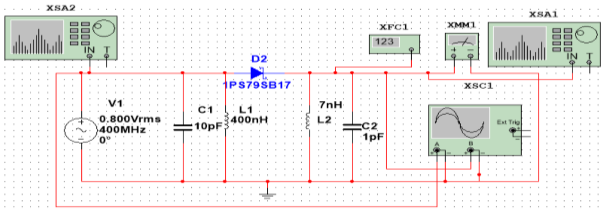

Fig. 5: Simulation Circuit Diagram of Frequency Doubling System Using Schottky Diode.

(A) (B)

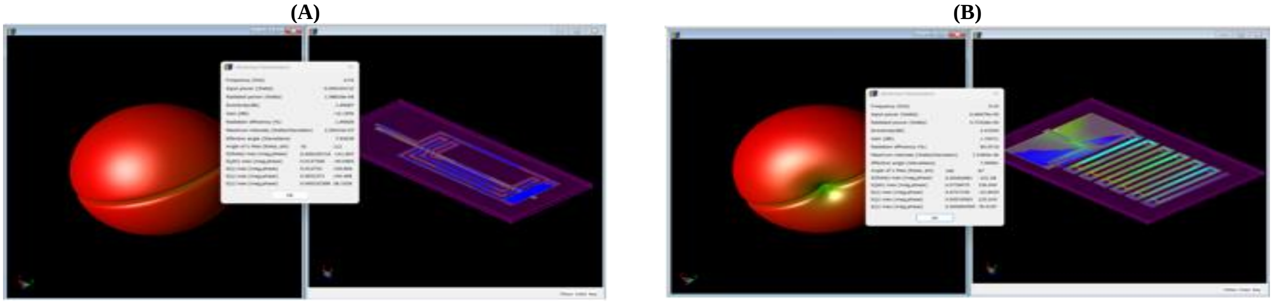

Fig. 6: 3-D Radiation Pattern with Gain in (DBI) and Current Distribution of A) Meander Line Monopole Antenna, B) Meander Line Antenna of 866 Mhz.

(A) (B)

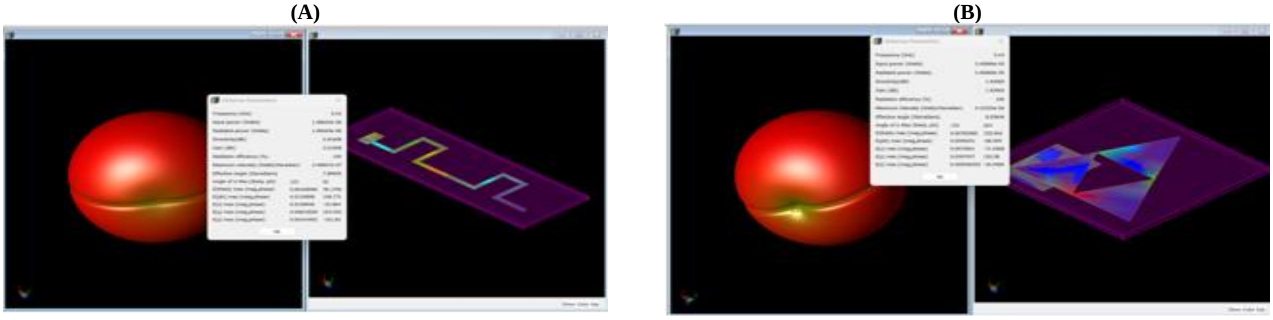

Fig. 7: 3-D Radiation Pattern with Gain In (DBI) and Current Distribution of A) Microstrip Antenna with Cohen-Minkowski Fractal, B) Microstrip Antenna with Triangle Fractal of 866 Mhz.

(A) (B)

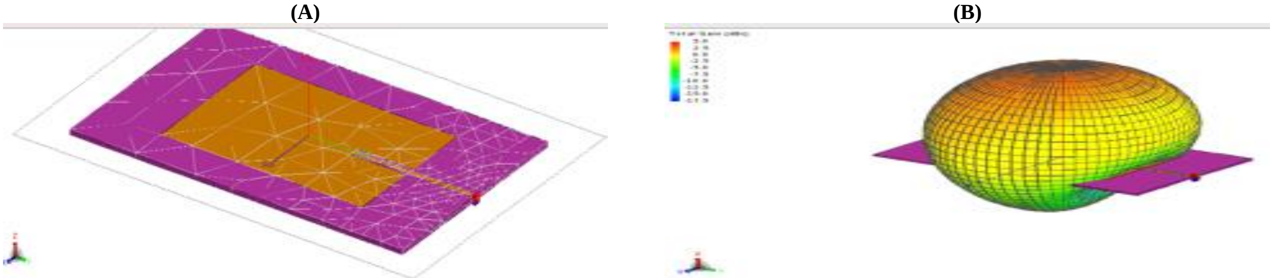

Fig. 8: A) Mf1 Microstrip Antenna, B) Simulated Radiation Pattern and Gain of Mf1 Microstrip Antenna for 866 Mhz.

The following table II represents the gain of different structures of Microstrip Patch Antenna of 866 Mhz. mF1 reflectenna is used to enhance the radiation pattern and redirect the radiated signal, improving the efficiency of signal transmission. Figure 9 shows a) graph of different Microstrip Patch Antenna gain for 433 MHz, b) graph of different Microstrip Patch Antenna gain for 866 MHz.

Table 2: Represents Gain of Different Structures of Microstrip Patch Antenna of 866Mhz

Antenna Structure	Gain (DBI)
Meander Line Monopole Antenna	1.99
Meander Line Antenna	1.53
Microstrip Antenna with Cohen-Minkowski Fractal	2.01
Microstrip Antenna with Triangle Fractal	1.93
Microstrip Patch Antenna	5.30

(A) (B)

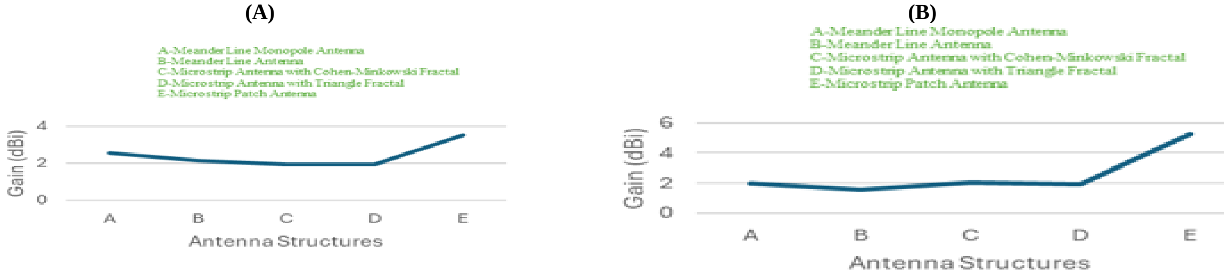

Fig. 9: Gain of Difference for Different Types of A) Microstrip Patch Antenna for 433 Mhz, B) Microstrip Patch Antenna for 866 Mhz.

The design parameters, including patch dimensions, metamaterial properties, and reflecting surface characteristics, are optimized for maximum performance in IoT sensor networks. We evaluated the performance of the frequency doubling reflector using electromagnetic simulation software, such as ADS, CADFEKO. The following metrics are considered: Frequency Doubling Efficiency: The efficiency of converting the fundamental frequency to the doubled frequency. Bandwidth: The operational bandwidth of the reflecting at both the fundamental and doubled frequencies. Radiation Pattern: The directional characteristics of the radiated signal, including gain and beamwidth. Return Loss: The reflection characteristics at both operating frequencies. Size and Compactness: The physical dimensions of the reflectenna, ensure suitability for IoT applications.

(A) **(B)**

Fig. 10: Hardware Implementation of A) F1 Microstrip Antenna for 433 Mhz, B) Mf1 Microstrip Antenna for 866 Mhz.

Figure 10 represents the hardware implementation of a) F1 Microstrip antenna for 433 MHz. b) mF1 Microstrip antenna for 866 MHz. Figure 11 shows a) Hardware implementation of frequency doubler using Schottky diode, b) hardware fabrication and implementation of frequency doubling reflectenna. The hardware design of the wireless IoT interrogator includes a Transmitter, Receiver, controller, and Wireless Module. A Radio frequency (RF) transmitter that sends interrogation signals at specific frequencies. A receiver that captures the backscattered signals from the passive sensors and decodes the transmitted data. ESP32 for managing the interrogation process, controlling the transmitter/receiver, and processing data.

(A) **(B)**

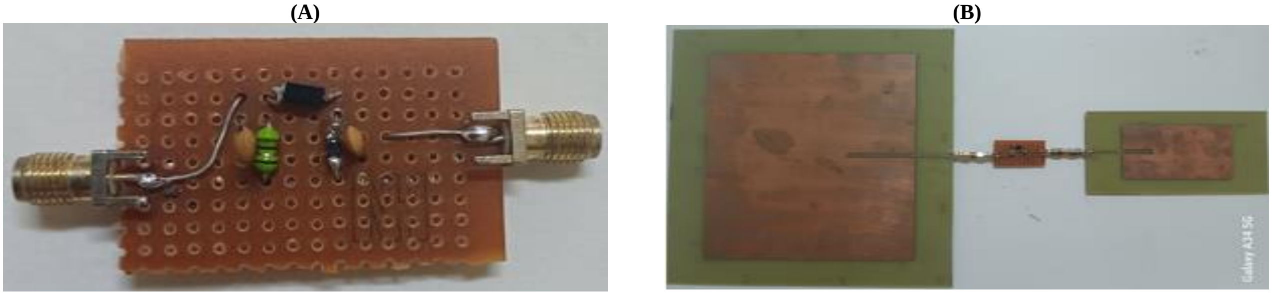

Fig. 11: Hardware Implementation of A) Frequency Doubler Using Schottky Diode, B) Frequency Doubling Reflectenna.

A module for communicating with the IoT platform or cloud-based infrastructure. The passive sensors are integrated with an FMC that receives the interrogation signal and reflects the signal to the interrogator. A system for managing data from multiple passive sensors, storing it in a database, and providing real-time analytics. The software system is designed to be compatible with common IoT platforms such as AWS IoT, ensuring seamless integration with cloud-based services for further data processing and analysis. Interrogator circuit for the production of an RF source, which will help Frequency frequency-doubling reflectenna to tune at the desired frequency. Figure 12 shows a) ESP32 with 433 MHz RFM95W LoRa, which will generate 433 MHz frequency, and b) ESP32 with 866 MHz RFM96 LoRa, which will act as an interrogator. The interrogator will receive an output signal, and further analysis will be made for the desired system requirements of IoT.

(A) **(B)**

Fig. 12: A) ESP32 with 433Mhz RFM95W Lora, B) ESP32 with 866Mhz RFM95W Lora.

4. Results analysis

We evaluate the performance of the wireless IoT interrogator through both simulations and real-world experiments. The key metrics measured include Communication Range, Data Throughput, and Gain of antenna. The maximum distance at which the interrogator can reliably communicate with passive sensors.

(A) (B)

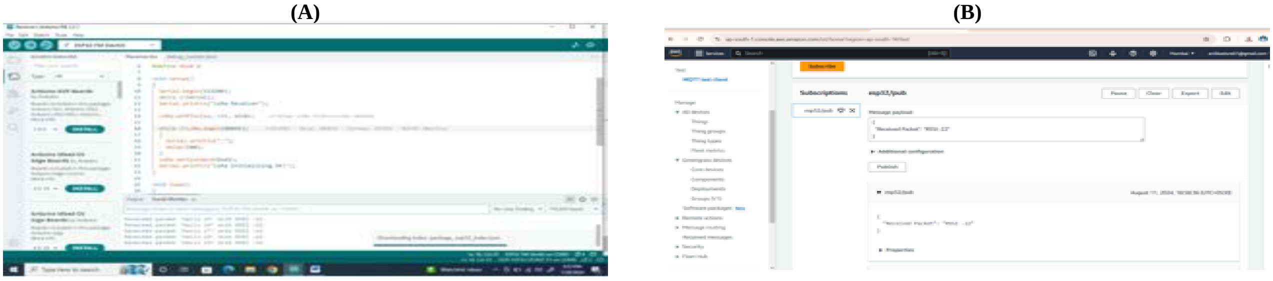

Fig. 13: A) ESP32 with 866 MHz RFM95W Lora Output, B) ESP32 with 866 MHz RFM95W Lora Output on AWS.

The rate at which data can be transmitted from the sensors to the IoT platform. The power consumption of the interrogator during various stages of operation. The time required for the interrogator to retrieve data from passive sensors and transmit it to the IoT platform. Hardware results show that the interrogator achieves a communication range of up to 100 meters in an open environment, with minimal energy consumption. Experimental results indicate a data throughput of 100 kbps and a latency of 10-15 milliseconds, which is sufficient for real-time IoT applications. Figure 13 shows ESP32 with 866 MHz RFM95W LoRa Output, b) ESP32 with 866 MHz RFM95W LoRa Output on AWS. Table III represents the Hardware output power for frequency frequency-doubling reflector system.

Table 3: Hardware Output Power for Frequency Doubling Reflectenna System

Operating Frequency at F1 Antenna	Distance between Tx and Rx	Operating Frequency at mF1 Antenna	Output Power
433Mhz	100cm	866Mhz	-20dB
433Mhz	200cm	866Mhz	-28dB
433Mhz	300cm	866Mhz	-36dB
433Mhz	400cm	866Mhz	-45dB
433Mhz	500cm	866Mhz	-55dB
433Mhz	600cm	866Mhz	-61dB
433Mhz	700cm	866Mhz	-70dB
433Mhz	800cm	866Mhz	-78dB
433Mhz	900cm	866Mhz	-86dB
433Mhz	1000cm	866Mhz	-89dB

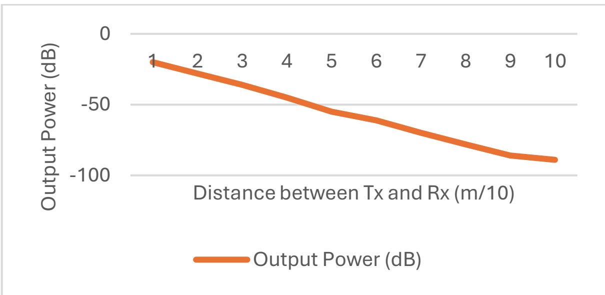

Fig. 14: Output Power for Frequency Doubling Reflectenna System.

Compared to traditional RFID readers, the proposed wireless IoT interrogator offers significant improvements in Energy Efficiency, Range, and Scalability. The interrogator minimizes energy usage while maintaining reliable communication. The system supports longer communication ranges and can handle a larger number of passive sensors, making it suitable for large-scale IoT deployments. Figure 14 shows a graph of output power for a frequency-doubling reflecting system.

5. Conclusion

The design and implementation of a wireless IoT interrogator for passive electromagnetic sensors are described in the paper. The proposed system is energy-efficient, scalable, and capable of supporting real-time data transmission to IoT networks, making it ideal for a wide range of IoT applications. F1 antenna gain is 3.50 dBi, and mF1 antenna gain is 5.10 dBi. Output power for frequency doubling reflectenna system observed -20dB, -89dB for distance between Tx and Rx at 100 cm, 1000cm, respectively. We analyze the system's performance through experiments, highlighting the interrogator's capability to support diverse IoT applications, such as environmental monitoring and smart agriculture. Future work will focus on Machine Learning for RSSI Analysis: Leveraging AI/ML techniques to enhance signal detection, optimization, and interference mitigation in IoT networks, improving the robustness of the system. Scalability and Multi-Node Networks: Exploring the scalability of the system to support multi-node networks and developing strategies to mitigate interference in large-scale IoT deployments.

References

[1] Anil M. Kasture, Kailash J. Karande, Shankar D. Nawale, "Performance Analysis of Various Nonlinear Elements in Frequency Multiplying Circuits for Wireless Applications". IJEER 12(4), 1332-1336. https://doi.org/10.37391/ijeer.120425.

[2] Anil M. Kasture, Kailash J. Karande, Shankar D. Nawale, Alttaf O. Mulani, "Design and analysis of planar frequency doubling reflectenna for IoT sensor networks", Comm. Appl. Nonlinear Anal., vol. 32, no. 9s, pp. 2279–2289, Mar. 2025. https://doi.org/10.37391/ijeer.120425.

[3] Anil M Kasture, Kailash J Karande "Comprehensive survey on passive wireless sensing technology for wireless application" Volume 2494, Issue 1, 31 October 2022, AIP Conf. Proc. 2494, 070013 (2022) https://doi.org/10.1063/5.0106945.

[4] M. Kasture, K. J. Karande and S. D. Nawale, "Optimization of Harmonic Generation in Frequency Multiplying Circuit for Wireless Application," 2024 3rd Edition of IEEE Delhi Section Flagship Conference (DELCON), New Delhi, India, 2024, pp. 1-5, https://doi.org/10.1109/DELCON64804.2024.10866239.

[5] E. García, A. Andújar, and J. Anguera, 'Antenna booster element for multiband operation', *Sensors (Basel)*, vol. 24, no. 9, Apr. 2024. https://doi.org/10.3390/s24092867.

[6] L. Anchidin, A. Lavric, P.-M. Mutescu, A. I. Petrariu, and V. Popa, 'The design and development of a microstrip antenna for Internet of Things applications', *Sensors (Basel)*, vol. 23, no. 3, p. 1062, Jan. 2023. https://doi.org/10.3390/s23031062.

[7] D. H. Abdulzahra, F. Alnahwi, A. S. Abdullah, Y. I. A. Al-Yasir, and R. A. Abd-Alhameed, 'A miniaturized triple-band antenna based on square split ring for IoT applications', *Electronics (Basel)*, vol. 11, no. 18, p. 2818, Sep. 2022. https://doi.org/10.3390/electronics11182818.

[8] B. Satriobudi, Iskandar and A. Mustafa, "IOT PROTOTYPE AIR QUALITY MONITORING USING LORA COMMUNICATION SYSTEM ON FREQUENCY 433 MHZ", 2022 16th International Conference on Telecommunication Systems, Services, and Applications (TSSA), Lombok, Indonesia, 2022, pp. 1-5, https://doi.org/10.1109/TSSA56819.2022.10063914.

[9] Zhang, L., Yang, H., Wang, Y., Zhang, S., & Ding, T. (2024), "Miniaturized active-frequency selective surfaces for low-power Internet of Things devices", Micromachines, 15(6), 736. https://doi.org/10.3390/mi15060736.

[10] W. M. Abdulkawi, A. F. A. Sheta, I. Elshafiey, and M. A. Alkanhal, 'Design of low-profile single- and dual-band antennas for IoT applications', *Electronics (Basel)*, vol. 10, no. 22, p. 2766, Nov. 2021. https://doi.org/10.3390/electronics10222766.

[11] S. Norlyana Azemi, N. K. Jiunn, M. Azmeer Kamarudin, C. Muhammad Nor Che Isa, and A. Amir, 'An Ultra-wideband CPW fed slot antenna for IoT Applications', *J. Phys. Conf. Ser.*, vol. 1755, no. 1, p. 012029, Feb. 2021. https://doi.org/10.1088/1742-6596/1755/1/012029.

[12] J. Colaco and R. B. Lohani, 'Metamaterial based multiband microstrip patch antenna for 5G wireless technology-enabled IoT devices and its applications', *J. Phys. Conf. Ser.*, vol. 2070, no. 1, p. 012116, Nov. 2021. https://doi.org/10.1088/1742-6596/2070/1/012116.

[13] Z. Mahlaoui, E. Antonino-Daviu, and M. Ferrando-Bataller, 'Radiation pattern reconfigurable antenna for IoT devices', *Int. J. Antennas Propag.*, vol. 2021, pp. 1–13, Aug. 2021. https://doi.org/10.1155/2021/5534063.

[14] D. T. T. Tu and N. V. Sang, 'Frequency reconfigurable multiband MIMO antenna base on gradient arcs for IoT devices', *Adv. Electromagn.*, vol. 10, no. 2, pp. 85–93, Oct. 2021. https://doi.org/10.1155/2021/5534063.

[15] D. Boukern, A. Bouacha, D. Aissaoui, M. Belazzoug, and T. A. Denidni, 'High-gain cavity antenna combining AMC-reflector and FSS superstrate technique', *Int. J. RF Microw. Comput-Aid. Eng.*, vol. 31, no. 7, Jul. 2021. https://doi.org/10.1002/mmce.22674.

[16] S. Thiruvenkadam, E. Parthasarathy, S. K. Palaniswamy, S. Kumar, and L. Wang, 'Design and performance analysis of a compact planar MIMO antenna for IoT applications', *Sensors (Basel)*, vol. 21, no. 23, p. 7909, Nov. 2021. https://doi.org/10.3390/s21237909.

[17] R. K. Saraswat and M. Kumar, 'Design and implementation of a multiband metamaterial-loaded reconfigurable antenna for wireless applications', *Int. J. Antennas Propag.*, vol. 2021, pp. 1–21, Dec. 2021. https://doi.org/10.1155/2021/3888563.

[18] K. Akhil, A. Sudeer, S. Nagendram, and S. S. S. Kalyan, 'Design of a dual band miniature microstrip patch antenna', *J. Phys. Conf. Ser.*, vol. 1804, no. 1, p. 012199, Feb. 2021. https://doi.org/10.1155/2021/3888563.

[19] P. P. Singh, P. K. Goswami, S. K. Sharma, and G. Goswami, 'Frequency reconfigurable multiband antenna for iot applications in wlan, WI-max, and c-band', *Prog. Electromagn. Res. C Pier C.*, vol. 102, pp. 149–162, 2020. https://doi.org/10.2528/PIERC20022503.

[20] G. Immadi *et al.*, 'Analysis of substrateintegrated frequency selective surface antenna for IoT applications', *Indones. J. Electr. Eng. Comput. Sci.*, vol. 18, no. 2, p. 875, May 2020. https://doi.org/10.11591/ijeecs.v18.i2.pp875-881.

[21] Ramos, T. Varum, and J. N. Matos, 'Compact N-band tree-shaped multiplexer-based antenna structures for 5G/IoT mobile devices', *Sensors (Basel)*, vol. 20, no. 21, p. 6366, Nov. 2020. https://doi.org/10.11591/ijeecs.v18.i2.pp875-881.

[22] V. K. Allam, B. T. P. Madhav, T. Anilkumar, and S. Maloji, 'A novel reconfigurable bandpass filtering antenna for iot communication applications', *Prog. Electromagn. Res. C Pier C.*, vol. 96, pp. 13–26, 2019. https://doi.org/10.2528/PIERC19070805.

[23] P. K. Goswami and G. Goswami, 'Trident shape ultra-large band fractal slot ebg antenna for multipurpose iot applications', *Prog. Electromagn. Res. C Pier C.*, vol. 96, pp. 73–85, 2019. https://doi.org/10.2528/PIERC19073002.

[24] N. AL-Fadhali *et al.*, 'Substrate integrated waveguide cavity backed frequency reconfigurable antenna for cognitive radio applies to internet of things applications', *Int. J. RF Microw. Comput-Aid. Eng.*, vol. 30, no. 1, Jan. 2020. https://doi.org/10.1002/mmce.22020.

[25] S. W. Y. Mung, C. Y. Cheung, K. M. Wu, and J. S. M. Yuen, 'Wideband rectangular foldable and non-foldable antenna for Internet of Things applications', *Int. J. Antennas Propag.*, vol. 2019, pp. 1–5, May 2019. https://doi.org/10.1155/2019/2125713.

[26] https://www.iexplainall.com/2020/05/design-equations-of-rectangular.html.